JGR Atmospheres

RESEARCH ARTICLE
10.1029/2019JD031029

Impacts of Observation Errors on Hurricane Forecasts When Assimilating Hyperspectral Infrared Sounder Radiances in Partially Cloudy Skies

Pei Wang[1], Jun Li[1], Zhenglong Li[1], Agnes H. N. Lim[1], Jinlong Li[1], and Mitchell D. Goldberg[2]

[1]Cooperative Institute for Meteorological Satellite Studies, University of Wisconsin-Madison, Madison, WI, USA, [2]NOAA JPSS Program Office, Lanham, MD, USA

Key Points:

- The noise amplification estimation of cloud-cleared radiances is established for hyperspectral infrared radiance assimilation in cloudy sky
- The appropriately inflated observation errors for VIIRS-based CrIS cloud-cleared radiances have a positive impact on hurricane forecasts
- The adjustments on temperature and geopotential height fields improve the simulation of hurricane structure and thus improve the forecast

Correspondence to:
J. Li,
jun.li@ssec.wisc.edu

Citation:
Wang, P., Li, J., Li, Z., Lim, A. H. N., Li, J., & Goldberg, M. D. (2019). Impacts of observation errors on hurricane forecasts when assimilating hyperspectral infrared sounder radiances in partially cloudy skies. *Journal of Geophysical Research: Atmospheres*, *124,* 10,802–10,813. https://doi.org/10.1029/2019JD031029

Received 16 MAY 2019
Accepted 28 AUG 2019
Accepted article online 15 SEP 2019
Published online 30 OCT 2019

Abstract Hyperspectral infrared (IR) sounders provide high vertical resolution atmospheric sounding information that can improve the forecast accuracy of numerical weather prediction (NWP) models. Due to the challenges of assimilating cloudy radiances, NWP centers usually assimilate only radiances that are not affected by clouds. An imager based cloud-clearing technique provides an alternative and effective way to remove the cloud effects from a partially cloudy field-of-view and derive the equivalent clear sky radiances or the cloud-cleared radiances (CCRs) for assimilation in NWP. Since the observation error is amplified in the cloud-clearing, or noise amplification process, it is necessary to inflate the observation errors appropriately in order to achieve the optimal value-added impact from assimilating CCRs. The estimation of observation error inflation is established and discussed. Hurricane Harvey (2017) and Hurricane Maria (2017) are used to simulate and understand the impacts of observation error inflation on the assimilation of Cross-track Infrared Sounder CCRs for hurricane forecast improvement. Both the precipitation location and intensity forecasts are improved when assimilating CCRs with an inflated observation error for Hurricane Harvey (2017). Assimilating CCRs with an inflated observation error adjusts the temperature and geopotential height fields and further affects the hurricane structures to improve the hurricane track forecasts, thereby demonstrating the importance of using hyperspectral IR measurements in partially cloudy skies for simulating the hurricane structure and improving its forecast. This method can be applied to other imager/sounder combined observations for improving sounder radiance assimilation in cloudy skies and has potential for operational applications.

1. Introduction

Satellite information has become one of the dominant sources for improving numerical weather prediction (NWP) model-based forecasts. In the last few years, all-sky satellite-based microwave sounder data have shown great benefit to forecast improvement at operational NWP systems (Bauer et al., 2010; Geer et al., 2017; Zhu et al., 2016) and in the research community (Li et al., 2016; Yang et al., 2016; Zhang et al., 2013). Infrared (IR) radiances, however, are often not fed into the assimilation system because a large percentage of those data are contaminated with clouds (Eresmaa, 2014; Wang et al., 2014). Typically, only radiances unaffected by clouds are effectively assimilated (McCarty et al., 2009; McNally, 2009). Direct assimilation of IR cloudy radiances remains challenging (Li et al., 2016). Further, the non-Gaussian distributed errors can degrade the impacts of the data assimilation (Pires et al., 2010).

A cloud-clearing (CC) method is introduced to support IR data assimilation by better utilizing the thermodynamic information under partially cloudy skies (Li et al., 2005; Reale et al., 2018; Wang et al., 2015, 2017). The CC method removes the cloud effects from a partially cloudy field of view (FOV) and calculates the clear sky equivalent using radiance data from an IR imager. The CC method has been successfully applied on the Atmospheric Infrared Sounder (AIRS) with help from the Moderate Resolution Imaging Spectroradiometer to obtain the AIRS cloud-cleared radiances (CCRs) and on the Cross-track Infrared Sounder (CrIS) with help from the Visible Infrared Imaging Radiometer Suite (VIIRS) to obtain the CrIS CCRs. The assimilation of cloud-cleared IR radiances has improved tropical cyclone forecasts in both regional and global models (Reale et al., 2018; Wang et al., 2015).

IR satellite radiance observation errors are an important factor in determining the effectiveness of the IR assimilation. The observations, radiative transfer model, and NWP background have a strong dependence on cloudiness. Geer and Bauer (2011) showed that the standard deviations (STDs) of differences between the first guess and observations are about (or nearly) 2 K in clear skies, but in cloudy or precipitation regions, the errors increase to 20 K, which is due, in part, to the RT and NWP model errors on cloudiness. Minamide and Zhang (2017) applied an adaptive observation error inflation technique for assimilating all-sky satellite brightness temperatures (BTs) with the ensemble-based data assimilation. In a previous study, CrIS CCRs were assimilated with the clear sky observation error (Wang et al., 2017). Since the noise is amplified during the CC process, the observation errors should, in principle, be inflated for optimal assimilation of the CCRs.

In this study, the VIIRS-based CC method (Li et al., 2005) is applied to CrIS data (with normal spectral resolution). The method for noise inflation is developed, and the noise amplification factor of CrIS CCRs is calculated. Hurricanes Harvey (2017) and Maria (2017), both of which made U.S. landfall, are selected as cases to show the impacts from the inflated observation errors of CrIS CCRs. This same method can be applied at operational centers for IR radiance assimilation in partially cloudy regions. Section 2 of this paper introduces the methodology for the noise amplification while the experimental design and data are explained in section 3. Finally, the impact study using CrIS CCRs with original clear observation errors and with inflated observation errors for hurricane track and precipitation forecasts are shown in section 4.

2. Methodology

The CC method is designed to extract the clear regions from the partially cloudy regions, using additional information to calculate the equivalent clear radiances for the partially cloudy FOVs. Depending on the sources of the additional information, there are three ways to obtain the IR CCRs. They can be obtained from (1) microwave radiances (Susskind et al., 2006), (2) NWP model background (Liu et al., 2016), and (3) high-resolution IR imager (Li et al., 2005). In this study, the method is based on observations only, no background information is needed, and it can also keep the original resolution of the IR sounder radiances. Since the third method has been demonstrated successfully with AIRS/Moderate Resolution Imaging Spectroradiometer and CrIS/VIIRS, it is used in this study. The imager-based CC method has been proven to be effective in getting thermodynamic information under partially cloudy skies. Assimilating these CCRs has further demonstrated a positive outcome on improving high impact weather forecasts (Wang et al., 2015, 2017).

In the previous study, the IR CCRs were assimilated as clear radiances, meaning the observation errors were set up as clear sky. However, the CCR noise is amplified during the CC process, so the observation errors of CCRs should be inflated as well. Based on the methodology to calculate CCRs (Li et al., 2005), the CCR can be derived from

$$R_v^{CC} = \frac{R_v^1 - R_v^2 N^*}{1 - N^*}, \tag{1}$$

where R_v^1 and R_v^2 are the cloudy radiances from two adjacent FOVs. As a function of wavenumber v, N^* is the ratio of the cloud effective coverage of the two FOVs, derived from combining sounder cloudy radiances and collocated imager clear sky radiances using an optimal estimation method where R_v^{CC} is the CCR. The R_v^1 and R_v^2 can be expressed as

$$R_v^1 = \overline{R_v^1} + R_v^{1'}, \tag{2}$$

$$R_v^2 = \overline{R_v^2} + R_v^{2'}, \tag{3}$$

where $\overline{R_v^1}$ and $\overline{R_v^2}$ are the truth of R_v^1 and R_v^2, and $R_v^{1'}$ and $R_v^{2'}$ are the noise of the R_v^1 and R_v^2, respectively. Therefore, the cloud-cleared spectrum can be written as

$$R_v^{CC} = \frac{\overline{R_v^1} + R_v^{1'} - \left(\overline{R_v^2} + R_v^{2'}\right) N^*}{1 - N^*}. \tag{4}$$

The noise of the R_v^{CC} can be calculated using

$$R_v^{CC'} = \sqrt{\left(\frac{R_v^{1'} - R_v^{2'}N^*}{1-N^*}\right)^2}. \quad (5)$$

The noise level of the two FOVs is assumed to be the same value, and the noise of the two FOVs is uncorrelated (which indicates that $\overline{R_v^{1'}R_v^{2'}} = 0$). Then the CCR noise amplification factor can be calculated using

$$\gamma = \sqrt{\frac{R_v^{1'2} - 2R_v^{1'}R_v^{2'}N^* + R_v^{2'2}N^{*2}}{\left(1-N^*\right)^2}} = \sqrt{\frac{1+N^{*2}}{\left(1-N^*\right)^2}}. \quad (6)$$

Equation (6) shows that the amplification is highly sensitive to N^*. When N^* is close to 1, the noise is significantly amplified, making the CCR highly noisy. In particular, when N^* is 1, there is infinite noise amplification. As a result, it is impossible to derive CCRs when the two FOVs are identical. Therefore, a radiance contrast between two adjacent FOVs is required to obtain accurate CCRs. In the CC process, any CCRs with N^* between 0.25 and 4 are flagged as failed due to extremely large noise levels. In this study, the observation errors of CCRs are inflated from the original clear observation error covariance based on (6). Since N^* is either smaller than 0.25 or larger than 4, the observation error is amplified to a value between 1 and 1.37. In the extreme clear sky situation ($N^* = 0$), the amplification will become one, meaning no error inflation.

In this study, the CC method is applied to CrIS radiances to calculate the CrIS CCRs. For CrIS CCR data, the observation errors are inflated based on equation (6) when CCRs are assimilated in the data assimilation system. The following experiments compare the results among the original CrIS data, CrIS CCRs with normal clear sky observation errors, and the CrIS CCRs with inflated observation errors.

3. Models, Experimental Design, and Hurricanes

3.1. DTC-GSI System and WRF-ARW Model

In this study, the Developmental Testbed Center (DTC) Gridpoint Statistical Interpolation (GSI) version 3.3 is used as the data assimilation system. The GSI is developed by NOAA/NASA, and the community version is supported by DTC. Because it can assimilate many kinds of observations, including conventional data, satellite radiances, satellite winds, and radar data, among others, it is widely used in the data assimilation research community (Han et al., 2016; Lim et al., 2014; Lin et al., 2017). The GSI 3-D Var method is used in this study. The background and observation errors are based on the North American Mesoscale Forecast System (NAM) regional model, and the radiance bias correction (BC) uses the enhanced BC method (Zhu et al., 2014), which is updated every cycle from the initial global model satellite bias coefficient.

The advanced research version of the Weather Research and Forecasting (WRF-ARW) model version 3.6.1 is used as the regional NWP model. The WRF-ARW model is designed for both operational forecasts and research studies. The horizontal resolution is 12 km with 400 × 300 grid points for Hurricane Harvey (2017) and 400 × 350 for Hurricane Maria (2017), while the vertical levels are 50 layers from the surface to 10 hPa for both hurricanes. In the WRF-ARW, several physical schemes are available for various research purposes. This study uses the following schemas: the WRF single-moment 6-class for the microphysics scheme, RRTMG for longwave and shortwave radiation schemes, and the Kain-Fritsch for the cumulus parameterization scheme.

3.2. Experimental Design

To evaluate the impacts of the inflated observation errors of CrIS CCR data, three experiments are carried out and defined in Table 1. The control run (*CNTRL*) assimilates the Global Telecommunication System (GTS) data, Advanced Microwave Sounding Unit (AMSU-A) radiances, Infrared Atmospheric Sounding Interferometer (IASI), Advanced Technology Microwave Sounder (ATMS) radiances, and original CrIS radiances with the original observation errors. With the regional model top set at 10 hPa in this study, the total number of CrIS channels assimilated in the GSI system is 70 within the longwave IR band (670–780 cm^{-1}). AMSU-A instruments are onboard NOAA-15, NOAA-18, NOAA-19, Metop-A, and Metop-B.

Table 1
Experimental Design for CNTRL, CCR, and CCRi

Experiment	GTS	AMSU-A	IASI	ATMS	CrIS	CrIS CCRs Clear Obs Err	CrIS CCRs Inflated Obs Err
CNTRL	√	√	√	√	√		
CCR	√	√	√	√		√	
CCRi	√	√	√	√			√

IASI instruments are onboard Metop-A and Metop-B, while CrIS and ATMS are onboard Suomi-NPP. The original CrIS clear observation errors are from the statistics built into the GSI system. The observation errors of CrIS for the wavenumber between 670 and 780 cm^{-1} are between 0.5 and 2 K. And the observation error of CrIS channels with wavenumber larger than 780 cm^{-1} is 2 K. The IR sounder radiances assimilation is based on the method of McNally and Watts (2003) to reject the cloud-contaminated channels. The *CCR* assimilates the data based on the CNTRL but replaces the original CrIS data with the CrIS CCRs data by using the same clear observation errors. The CrIS CCRs data set includes both clear sky and cloud-cleared CrIS radiances. The third experiment *CCRi* uses the same data as CCR, but the observation errors of CrIS CCRs are inflated from the original clear observation errors.

For Hurricane Harvey (2017), the three experiments start from 0000 UTC 17 August, after which the data are assimilated every 6 hr and followed by a 72-hr forecast. The assimilation time period is from 0000 UTC 17 August to 1800 UTC 25 August, while the forecasts last until 1800 UTC 28 August. Because the intensity of Hurricane Harvey (2017) decreased to a tropical wave/disturbance between 20 August and 22 August, the forecast evaluation is from 1800 UTC 22 to 0000 UTC 25. The experiment schemes for Hurricane Maria (2017) are the same as Hurricane Harvey (2017) with a forecast time period from 0000 UTC 18 September to 1800 UTC 24 September.

1. *CNTRL*: GTS + AMSU-A + ATMS + CrIS
2. *CCR*: GTS + AMSU-A + ATMS + CrIS + CCRs with normal clear observation errors
3. *CCRi*: GTS: ATMS-A + ATMS + CrIS + CCRs with inflated observation errors

3.3. Hurricanes

Hurricane Harvey (2017) was a destructive tropical cyclone, reaching maximum winds of 59 m/s during its first landfall and dropping over 60 in. of precipitation in Texas. According to the Tropical Cyclone Report (Blake & Zelinsky, 2018), Harvey produced the most significant tropical cyclone rainfall event in U.S. history. It reached Category 3 hurricane status on 25 August while it approached the middle Texas coast and continued to intensify to a Category 4. At 0300 UTC 26 August, Harvey's center made landfall on the northern end of San José Island and then made a second landfall on the Texas mainland 3 hr later. Because the minimum sea level pressure was 937 mb with sustained winds of 115 kt when it landed, Hurricane Harvey (2017) left significant damage. Hurricane Harvey continued to move to Texas coast, making its final landfall in southwestern Louisiana at 0800 UTC 30 August. It slowly weakened to a tropical depression.

Hurricane Maria (2017) was the 15th hurricane in the Atlantic Ocean in 2017. It devastated the island of Dominica as a Category 5 hurricane and Puerto Rico as a strong Category 4 before moving northwest to the continental United States. At around 0000 UTC 28 September, Hurricane Maria (2017) turned northeastward and moved away from the U.S. coast. Due to the serious damage it caused to the islands of the northeastern Caribbean Sea, Hurricane Maria is the third costliest hurricane in U.S. history (Pashch et al., 2019).

4. Results and Discussion

4.1. CrIS Radiances BC

BC is an important step in satellite radiance assimilation. It is also very challenging for regional NWP models due to the limited model domain and the non-uniform distribution of satellite data. The observation minus background (OmB) yields the difference between the BT observations and the simulated BTs from the background fields, while the BT observations minus analysis (OmA) show the difference between the BT observations and the simulated BTs from the analysis fields after BC and data assimilation. The STD of OmB and

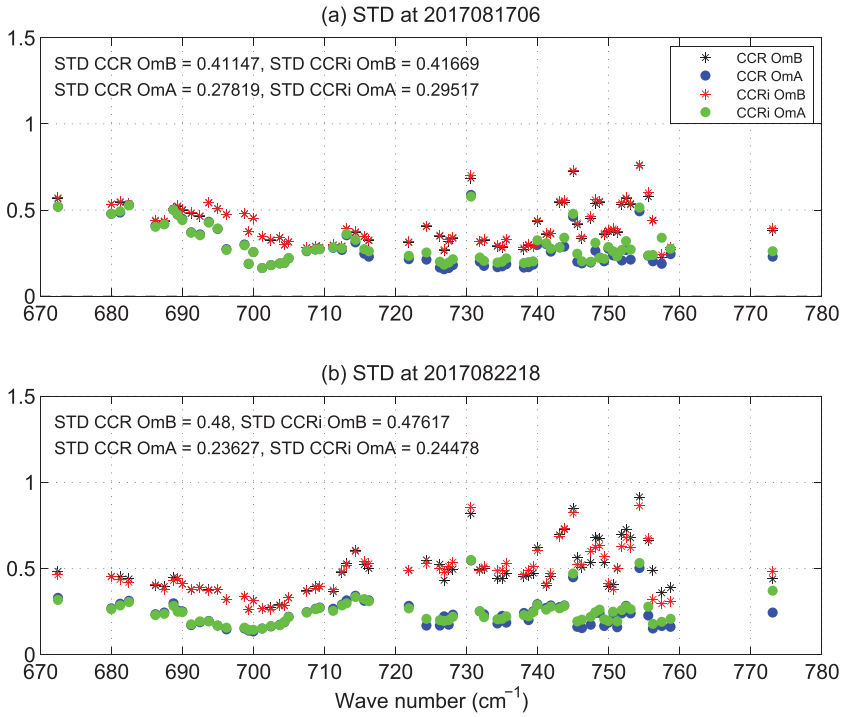

Figure 1. The STD of CCR OmB (black stars, unit: K), CCRi OmB (red stars, unit: K), CCR OmA (blue circles, unit: K), and CCRi OmA (green circles, unit: K) at (a) 0600 UTC 17 August and (b) 1800 UTC 22 August 2017.

OmA from CrIS observations is studied and shown in Figure 1. The STD at 0600 UTC 17 August (Figure 1a) reflects the differences at the beginning of the experiments. The observation errors are obtained from the global model at 0000 UTC 17 August, and the STD at 0600 UTC 17 August gives the STD distribution after the first analysis step for BC. The STD at 1800 UTC 22 August (Figure 1b) shows the STD after several steps in the assimilation along with updates. The STD of the OmA is much more stable at this time step.

Based on the STD of CrIS data for both the *CCR* and *CCR*i experiments at the two time steps, the STD of OmA is consistently smaller than the STD of OmB, indicating a great reduction in the difference between the observations and simulated BTs after CrIS and the other data assimilation. In general, the STD of OmA in *CCR*i is larger than that of OmA in *CCR*. At 0600 UTC 17 August, the STD of OmA in *CCR*i is about 5.8% larger than that of CCR, and at 1800 UTC 22 August, the STD of OmA in *CCR*i is about 3.8% larger than that of *CCR*. This result is expected and consistent with the inflated observation errors of *CCR*i. When observational errors increase, observational impact decreases, leading to the larger difference between the analysis and the observations.

4.2. Precipitation Verification for Hurricane Harvey (2017)

Based on the description of Hurricane Harvey (2017) as the most significant tropical cyclone rainfall event in U.S. history, its precipitation forecast is critical. The heavy rainfall occurred from 0000 UTC 26 to 0000 UTC 27 August across the Houston metro area. Accumulated precipitation from the three experiments is analyzed at 6-hr intervals to investigate the impact of CrIS data. The NCEP Stage IV multisensor quantitative precipitation values are used as observations with a resolution of 4 km. Stage IV analysis data include combined radar and river gauge data produced by the 12 River Forecast Centers over CONUS. The 6-hr accumulated precipitation between 0600 UTC 26 August and 1200 UTC 26 August is shown in Figure 2a. During this time Hurricane Harvey (2017) made landfall in Texas. At this point, the accumulated 6-hr precipitation is beyond 75 mm. The hurricane center is located at 28.7°N, 97.3°W. From the observations, the spiral rainfall pattern from the hurricane eye to the outside region is clearly defined. The heaviest precipitation occurred northeast of the hurricane center. Figure 2 also gives the simulated 6-hr accumulated precipitation from *CNTRL* (Figure 2b), from *CCR* (Figure 2c), and from *CCR*i (Figure 2d). The simulated resolution of 9 km is coarser

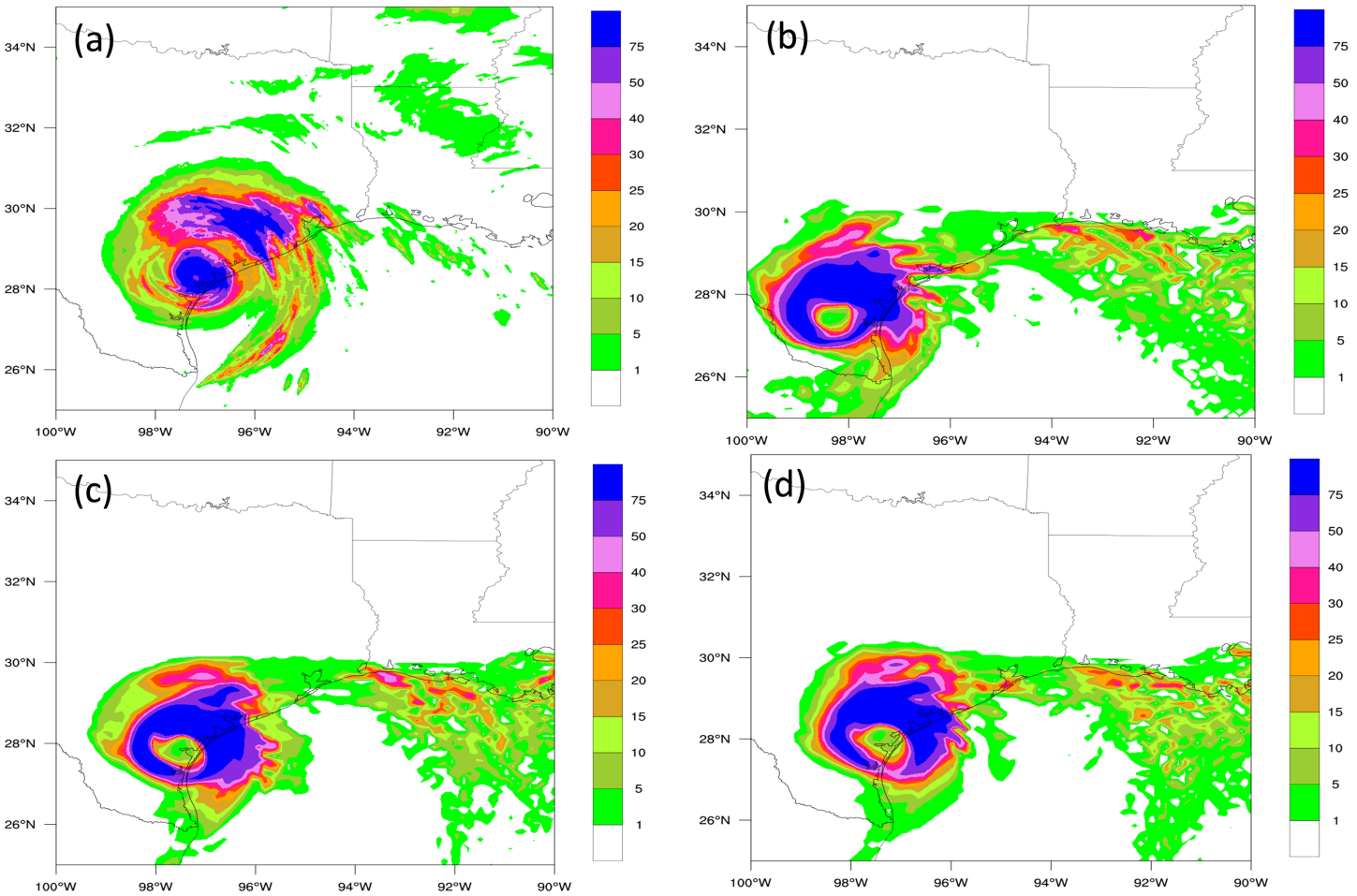

Figure 2. The accumulated precipitation (unit: mm) between 0600 UTC 26 August and 1200 UTC 26 August of Stage IV observations (a), CNTRL (b), CCR (c), and CCRi (d) from the forecast beginning at 0000 UTC 24 August 2017.

than the observation, resulting in a spiral rainfall pattern from simulated results that lacks clarity. However, the simulated precipitation also shows that the greatest precipitation amounts occur northeast of the hurricane center, which is consistent with the observations. The hurricane center of *CNTRL* (Figure 2b) is at 27.8°N, 98.4°W, southwest of the observation-based hurricane center, which indicates that the location of simulated precipitation is different from the observations. The distance between the hurricane center of *CNTRL* and the observation is about 147.05 km. Compared to the hurricane center from *CNTRL*, the hurricane centers of *CCR* (Figure 2c) and *CCR*i (Figure 2d) are very close to the observation-based hurricane center, with centers at 28.2°N, 97.8°W and 28.4°N, 97.6°W, respectively. The distance between the *CCR* hurricane center and the observation-based center is approximately 72.85 km, and the distance between the *CCRi* hurricane center and the observation-based center is approximately 44.40 km. Establishing a more accurate hurricane center can lead to a more accurate precipitation simulation. The accumulated precipitation of *CCR*i (Figure 2d) is closer to the observations than that of *CCR* (Figure 2c). The different forecast scores are based on the precipitation simulation discussed in the next section.

The equitable threat score (ETS) is an objective way to evaluate gridded precipitation forecasts (Ebert et al., 2007; Hamill, 1999; Wang et al., 2018). The ETS scores with 6-hr accumulated precipitation greater than 1, 10, 20, and 50 mm, respectively, are calculated for the three experiments during the forecasts on 0000 UTC 24 August, 2017 (Figure 3). The precipitation forecast is compared to the NCEP Stage IV multisensor quantitative precipitation analysis. Since the model domain resolution is coarser than observations, the Stage IV observations are interpolated to the model grid points, and then the ETS equation is applied to calculate the precipitation inside a box from 25°N to 35°N latitude and from 90°W to 100°W longitude. From the

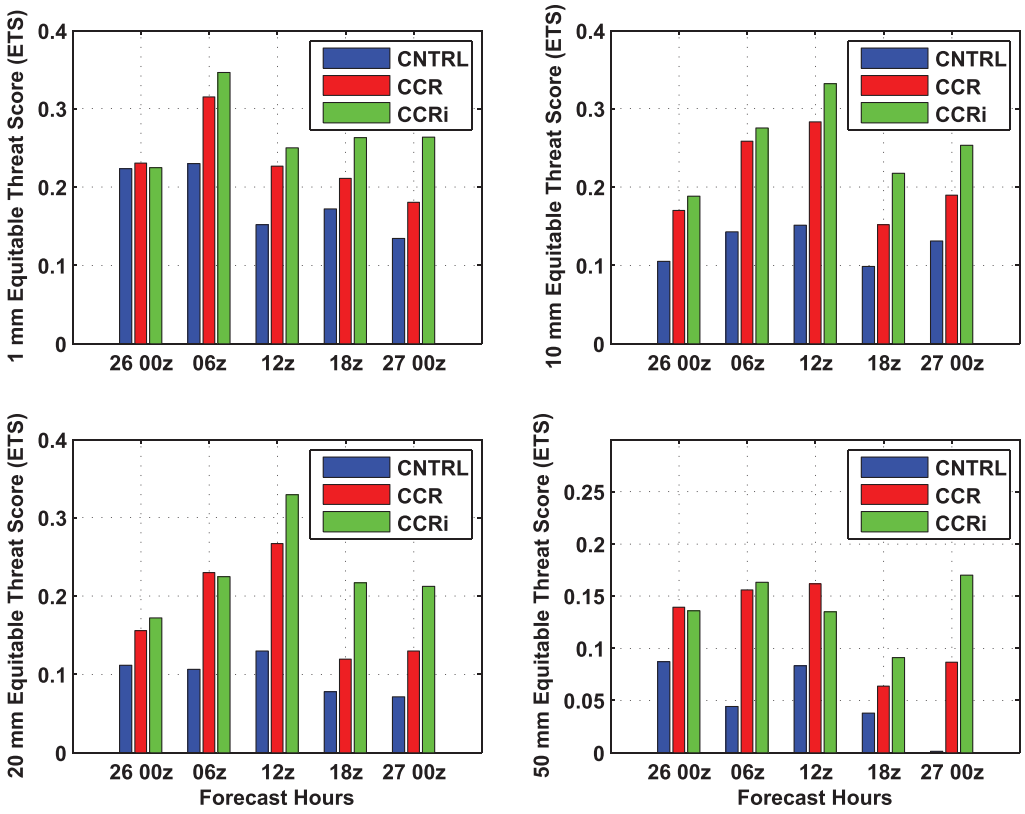

Figure 3. The ETS scores for CNTRL (blue), CCR (red), and CCRi (green) for 6-hr accumulated precipitation greater than or equal to 1 mm (upper left), 10 mm (upper right), 20 mm (lower left), and 50 mm (lower right), respectively, from the forecast beginning at 0000 UTC 24 August 2017.

results, the ETS scores of *CCR* and *CCR*i are consistently higher than the ETS scores of *CNTRL* for the entire period, indicating that the assimilation of CrIS CCRs can improve the precipitation forecast from the assimilation of original CrIS data only. In general, and particularly in the relative longer range forecast such as the forecast after 1200 UTC 26 August, the *CCR*i yields higher ETS scores than *CCR*, reflecting that the precipitation pattern of *CCR*i is closer to the observations from light to heavy rainfall. From the above ETS scores analysis and the discussion of the precipitation patterns, the results show that the assimilation of CrIS CCRs with inflated observation errors can improve the Harvey precipitation forecast for rainfall location and intensity.

4.3. Impact Analysis at 0000 UTC 24 August of Hurricane Harvey (2017) Forecasts

The heavy rainfall forecast from 0000 UTC 26 to 0000 UTC 27 August showed improvement with the assimilation of CrIS CCRs and the inflated observation errors. The temperature and geopotential heights at 500-hPa pressure level from the forecast beginning at 0000 UTC 24 August are plotted in Figure 4. Based on the geopotential height, the simulated hurricane centers are clearly defined. The structures of the three experiments are similar for the first 24-hr forecasts (Figures 4a–4c), but the warm core area of *CCR*i (Figure 4c) is the largest among them, which benefits the development of the tropical cyclone. The black star indicates the location of the hurricane centers in relation to the best track. At the 48-hr forecast, the *CNTRL* hurricane center is southwest of the best track center (Figure 4d), which is consistent with the precipitation pattern (Figure 2b). The distance between the *CNTRL* hurricane center and the observations increases at the 72-hr forecast (Figure 4g). The hurricane centers derived from *CCR* and *CCR*i are much closer to the observations than the *CNTRL* hurricane centers. The temperature field at the hurricane center from *CCR*i at the 48-hr forecast (Figure 4f) is more symmetric than from *CCR* (Figure 4e). At the 72-hr forecast, the hurricane center from *CCR*i (Figure 4i) is closest to the center of the best track among the three experiments. Based on the analysis of the atmospheric fields, the temperature structures directly affect the development of the

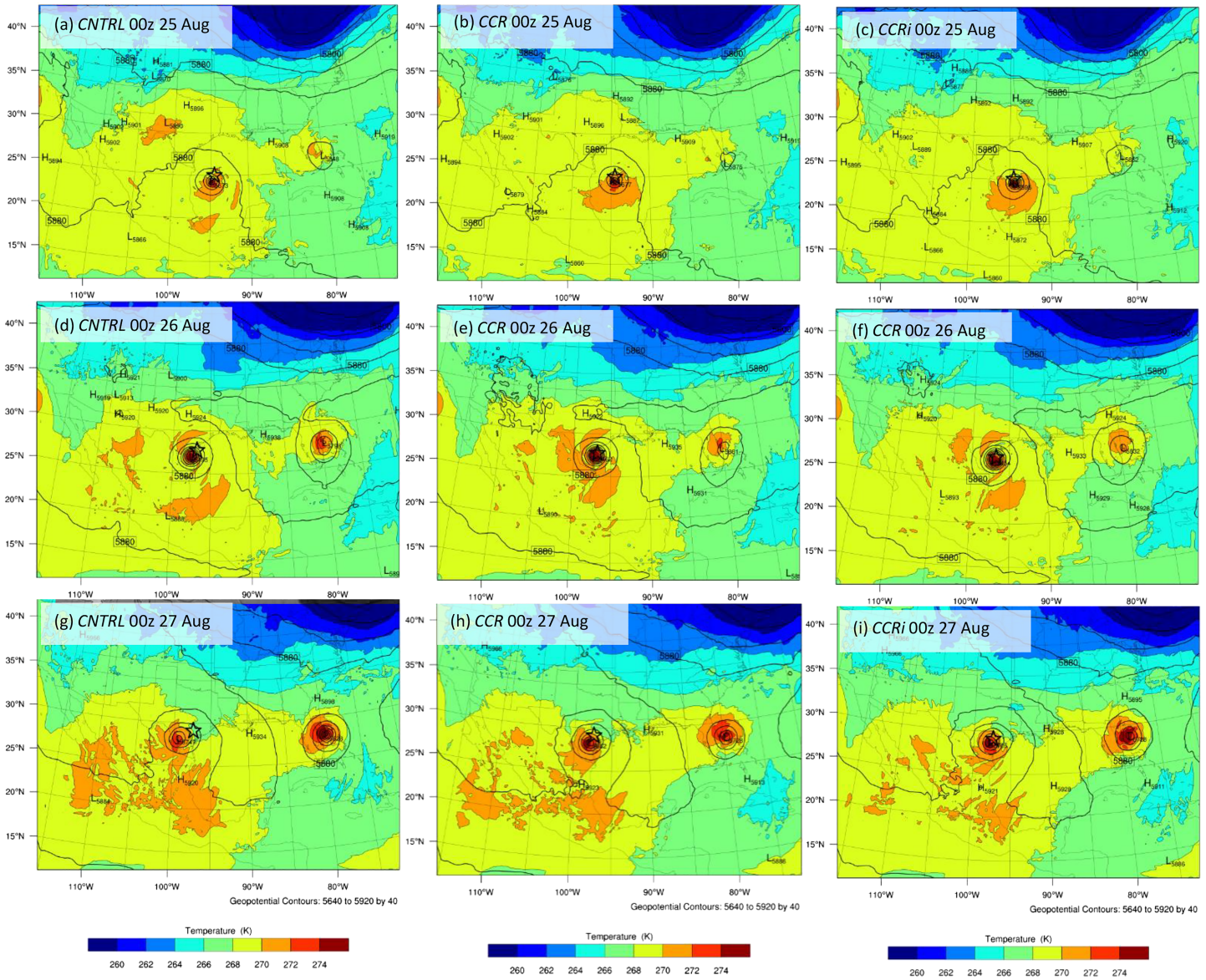

Figure 4. Temperature (shaded, unit: K), geopotential height (contour, unit: m^2/s^2), and wind vector at 500 hPa for 24-hr (a–c), 48-hr (d–f), and 72-hr (g–i) forecasts, respectively, from CNTRL (a, d, and g), from CCR (b, e, and h), and from CCRi (c, f, and i) at 0000 UTC 24 August 2017. The hurricane center from best track is marked as black star at each time.

tropical cyclones. Similar features are also found in the other levels. The assimilation of CCRs with inflated observation errors improves the hurricane forecast with improvement of the temperature fields. The more accurate track forecasts further affect the precipitation forecast, which makes the ETS of the heavy rainfall forecast from *CCRi* higher than the ETS of *CNTRL* and the ETS of *CCR* (Figure 3).

4.4. Hurricane Track and Intensity

Hurricane track and intensity forecasts are two important parameters necessary to verify hurricane forecasts. The hurricane track and minimum sea level pressure forecasts from the three experiments use the stand-alone Geophysical Fluid Dynamics Laboratory vortex tracker method. The "best tracks" for Hurricane Harvey (2017) and Hurricane Maria (2017) are from the National Hurricane Center Tropical Cyclone Report (Blake & Zelinsky, 2018; Pashch et al., 2019). The RMSE of the hurricane track and intensity between the best track and the experiments forecasts of Hurricane Harvey (2017) are plotted in Figure 5. For the

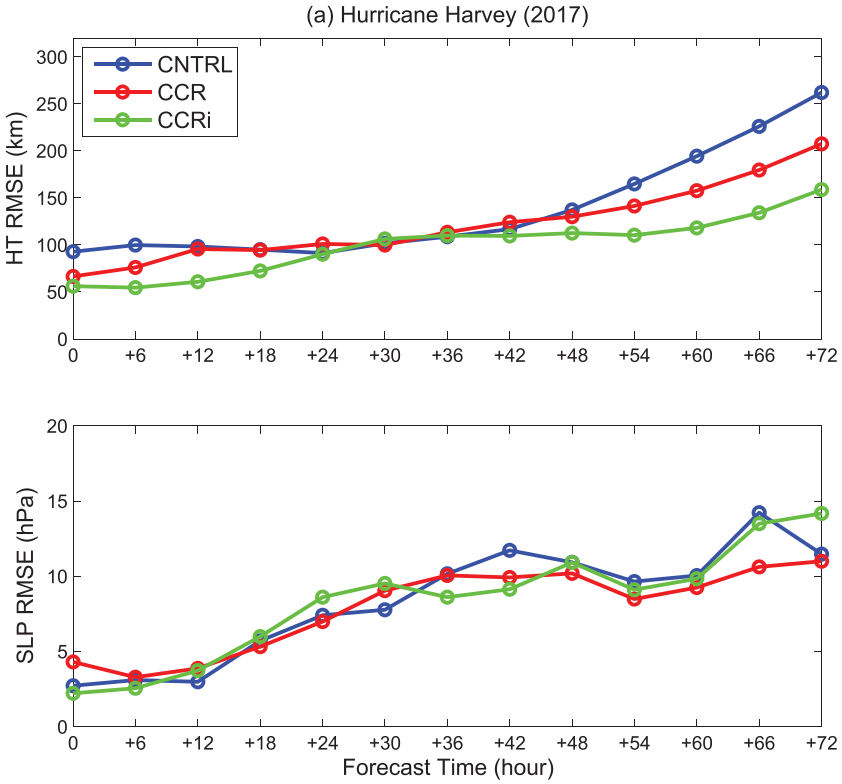

Figure 5. The hurricane track (top), and minimum sea level pressure (bottom) RMSE of the three experiments, CNTRL (blue), CCR (red), and CCRi (green), respectively, for all of the forecasts of Hurricane Harvey (2017).

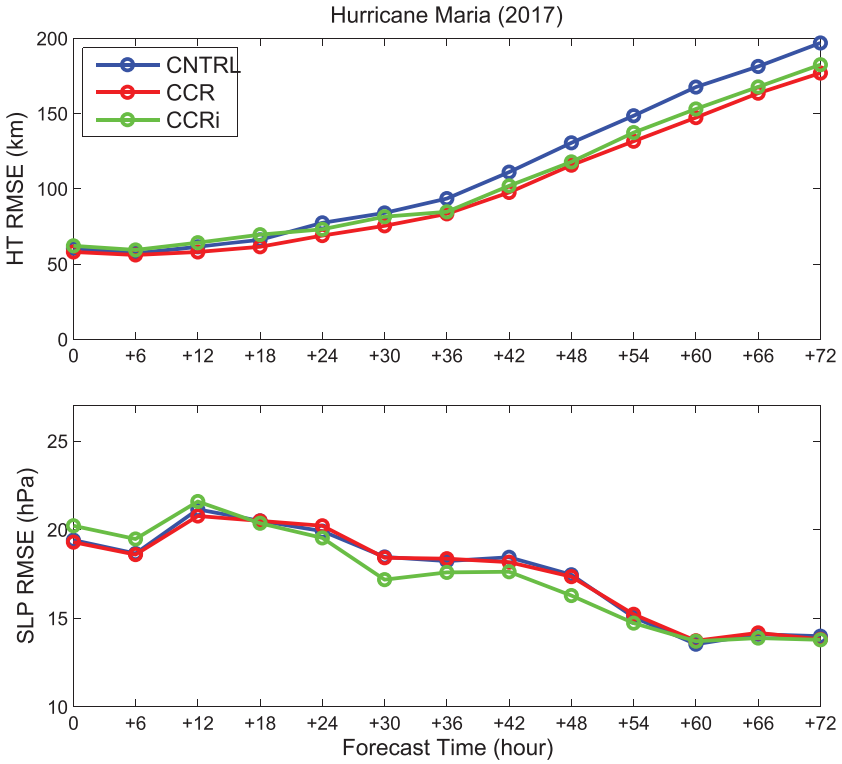

Figure 6. The same as Figure 5 but for Hurricane Maria (2017).

Table 2
The Improvement Ratio Between the CCR and CNTRL, and the Ratio Between CCRi and CNTRL (Unit: %) With Forecast Hours

Ratios	6 hr	12 hr	18 hr	24 hr	30 hr	36 hr
CCR	7.30%	0.48%	1.62%	−1.80%	−0.07%	−0.54%
CCRi	12.30%	7.65%	5.75%	0.32%	−0.69%	5.77%
	42 hr	48 hr	54 hr	60 hr	66 hr	72 hr
CCR	2.73%	3.39%	6.05%	6.77%	12.52%	7.47%
CCRi	9.61%	9.59%	13.30%	14.52%	16.35%	9.24%

hurricane track, the *CNTRL* produces the largest RMSE, and *CCR*i produces the smallest RMSE among the three experiments for the entire forecast time period. For the hurricane intensity forecasts, the three experiments have very comparable RMSE results. It is consistent with Hurricane Maria (2017) that the assimilation of *CCR*i can reduce the forecast error from *CNTRL* (Figure 6). However, the forecast error increases with the forecast time for each of the three experiments.

To further quantify the improvement in the hurricane forecasts, the improvement ratio of the two hurricanes is carried out for every 6-hr forecast. The improvement ratios are calculated as follows:

$$Improvment\ \ Ratio\ \ of\ \ CCR = \left(\frac{RMSE\ \ of\ \ CNTRL\ \ track - RMSE\ \ of\ \ CCR\ \ track}{RMSE\ \ of\ \ CNTRL\ \ track} \times \frac{1}{2} + \frac{RMSE\ \ of\ \ CNTRL\ \ intensity - RMSE\ \ of\ \ CCR\ \ intensity}{RMSE\ \ of\ \ CNTRL\ \ intensity} \times \frac{1}{2} \right) \times 100\%$$

$$Improvment\ \ Ratio\ \ of\ \ CCRi = \left(\frac{RMSE\ \ of\ \ CNTRL\ \ \ track - RMSE\ \ of\ \ CCRi\ \ track}{RMSE\ \ of\ \ CNTRL\ \ track} \times \frac{1}{2} + \frac{RMSE\ \ of\ \ CNTRL\ \ intensity - RMSE\ \ of\ \ CCRi\ \ intensity}{RMSE\ \ of\ \ CNTRL\ \ intensity} \times \frac{1}{2} \right) \times 100\%$$

A positive ratio represents that the RMSE of *CNTRL* is larger than that of *CCR* or *CCR*i, while a negative ratio represents that the RMSE of *CNTRL* is smaller than that of *CCR* or *CCR*i. Table 2 shows the improvement ratios for both Hurricane Harvey (2017) and Hurricane Maria (2017) together for the 72-hr forecast period. From Table 2, in general, the *CCR* and *CCR*i have more positive ratios than negative ratios. For *CCR*, negative ratios are for the 24-, 30-, and 36-hr forecasts, though the negative ratios are very small. For *CCR*i, however, negative ratios are only evident for the 30-hr forecast, which is due to the large RMSE of the intensity forecasts. For both *CCR* and *CCR*i, the ratios from the 42- to 72-hr forecasts are all positive, which indicates that starting from the 42-hr forecasts, both hurricane track and intensity forecasts are improved from the *CNTRL*. The positive value for *CCR*i is larger than *CCR* most of the time, which also illustrates that the inflated observation errors for assimilating CrIS CCRs are necessary and can further reduce the RMSE of hurricane track forecasts.

5. Summary

Assimilating IR radiances under cloudy skies continues to be challenging, but the CC method provides an alternative way to use the thermodynamic information under partially cloudy regions. During the CC processing, the observation noise is amplified for the CCRs compared with the original CrIS clear observations. Therefore, a noise amplification method is developed in this study, which applies the inflated observation errors for the assimilation of CrIS CCRs. The noise amplification is only related to the cloudiness of the two adjacent CrIS FOVs, and the inflated observation errors are only applied on the CrIS CCRs data.

Based on the analysis of the CrIS OmB and OmA, it is found that the STD of OmA from *CCR*i is larger than that from *CCR* for most channels, which is consistent with the inflated observation errors for the assimilation of VIIRS-based CrIS CCRs. To investigate the impacts of inflated observation errors, Hurricane Harvey (2017) and Hurricane Maria (2017) are used as case studies. Harvey produced the

most rainfall from a tropical cyclone in U.S. history. The heavy rainfall occurred during the period 0000 UTC 26 August to 0000 UTC 27 August. The temperature, geopotential height, and wind vectors are analyzed for the 72-hr forecasts. The ETS scores are calculated for every 6-hr forecast during this period from accumulated 1- to 50-mm precipitation. From the results, the ETS scores of *CCR* and *CCR*i are much higher than the ETS scores of *CNTRL* for the entire period, which indicates that the assimilation of CrIS CCRs can improve the precipitation forecasts. The ETS scores further show that the inflated CCR observation errors can improve the precipitation forecast for both the rainfall location and intensity of Hurricane Harvey (2017). The assimilation of CrIS CCRs with inflated observation errors also improves the hurricane track forecasts of Hurricane Harvey (2017) and Hurricane Maria (2017). The RMSE of the *CCR*i track is the smallest among the three experiments. These results demonstrate that the noise amplification method for the assimilation of IR sounder-based CCRs could benefit the hurricane forecasts by better representing the observation errors of CCR data. In the future, the CC method for CrIS data will be further applied on the full spectral resolution CrIS from SNPP and NOAA-20, and the inflated observation errors will also be used for the assimilation of full spectral resolution CrIS CCRs. This method can be applied to other imager/sounder combined observations (Li et al., 2004, 2005) for improving sounder radiance assimilation in partially cloudy skies and has potential for operational applications.

Acknowledgments

This work is supported by the JPSS Risk Reduction program and the NOAA GOES-R High Impact Weather (HIW) program. Thanks to the University of Wisconsin-Madison Cooperative Institute for Meteorological Satellite Studies (CIMSS) and the Space Science and Engineering Center (SSEC) sounding team for preparing the VIIRS-based CrIS cloud-cleared radiances and for access to the "S4" supercomputer at SSEC. The views, opinions, and findings contained in this report are those of the authors and should not be construed as an official National Oceanic and Atmospheric Administration or U.S. government position, policy, or decision. The precipitation observation data can be downloaded online (http://cdc.cma.gov.cn/sksj.do?method=ssrjscprh). The FNL reanalysis data, GTS data, AMSU-A, CrIS, and ATMS radiances are available from the NCAR/UCAR Research Data Archive (https://rda.ucar.edu/datasets/). The "best tracks" of Hurricane Harvey (2017) and Hurricane Maria (2017) are available from the NCAR/RAL Tropical Cyclone Guidance Project (http://hurricanes.ral.ucar.edu/).

References

Bauer, P., Geer, A. J., Lopez, P., & Salmond, D. (2010). Direct 4D-Var assimilation of all-sky radiances. Part I: Implementation. *Quarterly Journal of the Royal Meteorological Society*, *136*(652), 1868–1885. https://doi.org/10.1002/qj.659

Blake, E. S., & Zelinsky, D. A. (2018). Tropical Cyclone Report: Hurricane Harvey (AL092017). National Hurricane Center, 1-76.

Ebert, E. E., Janowiak, J. E., & Kidd, C. (2007). Comparison of near-real-time precipitation estimates from satellite observations and numerical models. *Bulletin of the American Meteorological Society*, *88*(1), 47–64. https://doi.org/10.1175/BAMS-88-1-47

Eresmaa, R. (2014). Imager-assisted cloud detection for assimilation of Infrared Atmospheric Sounding Interferometer radiances. *Quarterly Journal of the Royal Meteorological Society*, *140*(684), 2342–2352. https://doi.org/10.1002/qj.2304

Geer, A.,. J., Baordo, F., Bormann, N., Chambon, P., English, S. J., Kazumori, M., et al. (2017). The growing impact of satellite observations sensitive to humidity, cloud and precipitation. *Quarterly Journal of the Royal Meteorological Society*, *143*(709), 3189–3206. https://doi.org/10.1002/qj.3172

Geer, A. J., & Bauer, P. (2011). Observation errors in all-sky data assimilation. *Quarterly Journal of the Royal Meteorological Society*, *137*(661), 2024–2037. https://doi.org/10.1002/qj.830

Hamill, T. M. (1999). Hypothesis tests for evaluating numerical precipitation forecasts. *Weather and Forecasting*, *14*(2), 155–167. https://doi.org/10.1175/1520-0434(1999)014<0155:HTFENP>2.0.CO;2

Han, H., Li, J., Goldberg, M., Wang, P., Li, J., Li, Z., et al. (2016). Microwave sounder cloud detection using a collocated high-resolution imager and its impact on radiance assimilation in tropical cyclone forecasts. *Monthly Weather Review*, *144*(10), 3937–3959. https://doi.org/10.1175/MWR-D-15-0300.1

Li, J., Liu, C. Y., Huang, H.-L., Schmit, T. J., Menzel, W. P., & Gurka, J. (2005). Optimal cloud-clearing for AIRS radiances using MODIS. *IEEE Transactions on Geoscience and Remote Sensing*, *43*(6), 1266–1278. https://doi.org/10.1109/TGRS.2005.847795

Li, J., Menzel, W. P., Sun, F., Schmit, T. J., & Gurka, J. (2004). AIRS subpixel cloud characterization using MODIS cloud products. *Journal of Applied Meteorology*, *43*(8), 1083–1094. https://doi.org/10.1175/1520-0450(2004)043<1083:ASCCUM>2.0.CO;2

Li, J., Wang, P., Han, H., Li, J., & Zheng, J. (2016). On the assimilation of satellite sounder data in cloudy skies in numerical weather prediction models. *Journal of Meteorological Research*, *30*(2), 159–182. https://doi.org/10.1007/s13351-016-5114-2

Lim, A. H. N., Jung, J. A., Huang, H. A., Ackerman, S. A., & Otkin, J. A. (2014). Assimilation of clear sky Atmospheric Infrared Sounder radiances in short-term regional forecasts using community models. *Journal of Applied Remote Sensing*, *8*(1), 083655. https://doi.org/10.1117/1.JRS.8.083655

Lin, H., Weygandt, S. S., Lim, A. H. N., Hu, M., Brown, J. M., & Benjamin, S. G. (2017). Radiance preprocessing for assimilation in the Hourly Updating Rapid Refresh Mesoscale Model: A study using AIRS data. *Weather and Forecasting*, *32*(5), 1781–1800. https://doi.org/10.1175/WAF-D-17-0028.1

Liu, H., Collard, A., & Derber, J. C. (2016). Variational cloud-clearing with CrIS data at NCEP, AMS Annual Meeting, 10-14 January, 2016, New Orleans, LA.

McCarty, W., Jedlovec, G., & Miller, T. L. (2009). Impact of the assimilation of Atmospheric Infrared Sounder radiance measurements on short-term weather forecasts. *Journal of Geophysical Research*, *114*, D18122. https://doi.org/10.1029/2008JD011626

McNally, A. (2009). The direct assimilation of cloud-affected satellite infrared radiances in the ECMWF 4D-Var. *Quarterly Journal of the Royal Meteorological Society*, *135*(642), 1214–1229. https://doi.org/10.1002/qj.426

McNally, A., & Watts, P. (2003). A cloud detection algorithm for high-spectral-resolution infrared sounders. *Quarterly Journal of the Royal Meteorological Society*, *129*(595), 3411–3423. https://doi.org/10.1256/qj/02.208

Minamide, M., & Zhang, F. (2017). Adaptive observation error inflation for assimilating all-sky satellite radiance. *Monthly Weather Review*, *145*(3), 1063–1081. https://doi.org/10.1175/MWR-D-16-0257.1

Pashch, R. J., Penny, A. B., & Berg, R. (2019). Tropical Cyclone Report: Hurricane Maria (AL152017), National Hurricane Center, 1-48.

Pires, C. A., Talagrand, O., & Bocquet, M. (2010). Diagnosis and impacts of non-Gaussianity of innovations in data assimilation. *Physica D: Nonlinear Phenomena*, *239*(17), 1701–1717. https://doi.org/10.1016/j.physd.2010.05.006

Reale, O., McGrath-Spangler, E. L., McCarty, W., Holdaway, D., & Gelaro, R. (2018). Imapct of adaptively thinned AIRS cloud-cleared radiances on tropical cyclone representation in a global data assimilation and forecast system. *Weather and Forecasting*, *33*, 909–931. https://doi.org/10.1175/WAF-D-17-0175.1

Susskind, J., Barnet, C., Blaisdell, J., Iredell, L., Keita, F., Kouvaris, L., et al. (2006). Accuracy of geophysical parameters derived from Atmospheric Infrared Sounder/Advanced Microwave Sounding Unit as a function of fractional cloud cover. *Journal of Geophysical Research*, *111*, D09S17. https://doi.org/10.1029/2005JD006272

Wang, P., Li, J., Goldberg, M. D., Schmit, T. J., Lim, A. H. N., Li, Z., et al. (2015). Assimilation of thermodynamic information from advanced infrared sounders under partially cloudy skies for regional NWP. *Journal of Geophysical Research: Atmospheres*, *120*, 5469–5484. https://doi.org/10.1002/2014JD022976

Wang, P., Li, J., Li, J., Li, Z., Schmit, T. J., & Bai, W. (2014). Advanced infrared sounder subpixel cloud detection with imagers and its impact on radiance assimilation in NWP. *Geophysical Research Letters*, *41*, 1773–1780. https://doi.org/10.1002/2013GL059067

Wang, P., Li, J., Li, Z., Lim, A. H. N., Li, J., Schmit, T. J., & Goldberg, M. D. (2017). The impact of Cross-track Infrared Sounder (CrIS) cloud-cleared radiances on Hurricane Joaquin (2015) and Matthew (2016) forecasts. *Journal of Geophysical Research: Atmospheres*, *122*, 13,201–13,218. https://doi.org/10.1002/2017JD027515

Wang, P., Li, J., Lu, B., Schmit, T. J., Lu, J., Lee, Y. K., et al. (2018). Impact of moisture information from Advanced Himawari Imager Measurements on heavy precipitation forecasts in a regional NWP model. *Journal of Geophysical Research: Atmospheres*, *123*, 6022–6038. https://doi.org/10.1029/2017JD028012

Yang, C., Liu, Z., Bersch, J., Rizvi, S. R. H., Huang, X.-Y., & Min, J. (2016). AMSR2 all-sky radiance assimilation and its impact on the analysis and forecast of Hurricane Sandy with a limited-area data assimilation system. *Tellus A: Dynamic Meteorology and Oceanography*, *68*(1), 1–19. https://doi.org/10.3402/tellusa.v68.30917

Zhang, M., Zupanski, M., Kim, M.-J., & Knaff, J. A. (2013). Assimilating AMSU-A radiances in the TC core area with NOAA operational HWRF (2011) and a hybrid data assimilation system: Danielle (2010). *Monthly Weather Review*, *141*(11), 3889–3907. https://doi.org/10.1175/MWR-D-12-00340.1

Zhu, Y., Derber, J., Collard, A., Dee, D., Treadon, R., Gayno, G., & Jung, J. A. (2014). Enhanced radiance bias correction in the National Centers for Environmental Prediction's Gridpoint Statistical Interpolation data assimilation system. *Quarterly Journal of the Royal Meteorological Society*, *140*(682), 1479–1492. https://doi.org/10.1002/qj.2233

Zhu, Y., Liu, E., Mahajan, R., Thomas, C., Groff, D., van Delst, P., et al. (2016). All-sky microwave radiance assimilation in NCEP's GSI analysis system. *Monthly Weather Review*, *144*(12), 4709–4735. https://doi.org/10.1175/MWR-D-15-0445.1